FEATURE ARTICLE

Generic Schemes for Single-Molecule Kinetics. 1: Self-Consistent Pathway Solutions for Renewal Processes

Jianshu Cao* and Robert J. Silbey*

Department of Chemistry, Massachusetts Institute of Technology Cambridge, Massachusetts 02139

Received: April 17, 2008; Revised Manuscript Received: June 4, 2008

In this paper, we discuss a strategy for reducing a complex single molecule kinetic process to a set of generic structures (motifs) that are building blocks for a general kinetic scheme. In general, these motifs have complex kinetics (i.e., waiting time distribution functions) which are composed of fundamental kinetic steps. (1) First, we treat four different experimental single molecule measurements within both the usual kinetic framework (i.e., using the rate matrix) and the waiting time distribution function framework. The two frameworks are then shown to be equivalent and can be formulated on the basis of the first passage time distribution function of monitored single molecule events. (2) Second, to calculate this basic quantity, we decompose a complex kinetic scheme with the help of two kinetic motifs, sequential and branching, and derive self-consistent equations by convoluting waiting time distributions and first passage time distribution(s) along the reaction pathway(s). (3) As examples, two experimental systems, a chain reaction model with a special case of enzymatic reactions and a general kinetic model for fluorescence emission, are analyzed on the basis of a generic scheme composed of a monitored link, controlled link, and unknown link, each representing a possible subscheme associated with a complex waiting time distribution function. As a result, single molecule measurements of the generic scheme retain the same functional form when a kinetic link is altered within a subscheme, and different measurements can be classified and analyzed within the same framework. (4) Finally, to explore the physical reasons for nonexponential waiting time distribution, we use the example of blinking phenomena to discuss several scenarios of dynamic and static disorder and their implications for observed memory effects. The self-consistent pathway formalism is presented in this paper for renewal processes and will be generalized to nonrenewal processes with memory effects in a future publication.

I. Introduction

The advance of single molecule techniques has inspired recent interest in chemical kinetics, statistics, and data analysis.[1,2] Much of the current theoretical formulation of single molecule kinetics is built on the transfer matrix solution, which is standard for first-order kinetics[3] but which can be ineffective as the probed systems and proposed schemes become increasingly complex. From the viewpoint of theoretical analysis, for any changes in a subscheme, whether rising from mutations, different probes, or changes in experimental conditions, the standard calculation has to be repeated, making it difficult to predict the generic behavior of a broad class of schemes. From the viewpoint of numerical analysis, the lack of generic schemes for a class of single molecular measurements also causes difficulties in comparing different interpretations of single molecule data and defining a definite model for their information content.[4−7] To address these two issues, we propose a self-consistent solution based on single molecule reaction pathways to compute first-order kinetics, which will lead to the definition of the generic scheme, i.e., the irreducible scheme composed of monitored link(s), controlled link(s), and unknown link(s). The monitored link is the kinetic step or subscheme directly detected in single molecule experiments, the controlled link is the kinetic step or subscheme governed by experimental conditions, and the unknown link is the kinetic step or subscheme to be inferred with single molecule measurements. Our discussion in this paper is limited to renewal processes and will be further extended to nonrenewal processes.[8]

Our self-consistent reaction pathway solution is inspired by the original paper by Ninio on an alternative approach to deriving reaction rate constants in enzymatic reactions.[9] Instead of calculating average rate constants, we extend his approach to calculate the probability distribution function (PDF) of the first passage time $\phi(t)$,[10] i.e., the PDF of adjacent single molecule transition events, which allows the prediction of all single molecule measurements in a renewal process. Following the single molecule reaction pathways, we decompose a complex kinetic scheme into subschemes using kinetic motifs and convolute waiting time distributions and first passage time distributions along the pathways. Each kinetic loop (including reversible links) defines a self-consistent equation, which is solved to yield the waiting time distribution for the subscheme. By systematically concatenating the side-branches and chain reactions, we can reduce a complex scheme to its "backbone" or "skeleton", only constrained by the monitored link(s) and controlled link(s), and thus define the irreducible scheme, which corresponds to the maximal amount of information one can extract from single molecule data. Several groups have recently

* To whom correspondence should be addressed.

10.1021/jp803347m CCC: $40.75
Published on Web 09/25/2008

Bob Silbey received his Ph.D. at the University of Chicago working with Professor Stuart Rice, after which he worked as an AFOSR postdoctoral fellow with Professor Joseph Hirschfelder at the University of Wisconsin. He has spent his entire academic career as a faculty member at M.I.T., except for visiting professorships in The Netherlands, France, and Germany. Silbey has done research on energy and electron transfer in condensed phases, energy transfer from excited molecules to surfaces, electronic states and optical properties of conjugated polymers, quantum dynamics of tunneling systems interacting with their environment, the coupling of vibrational and electronic degrees of freedom in molecules and solids, and the quantum dynamics of highly excited molecules. He has worked very closely with experimentalists in all his research.

Jianshu Cao is an associate professor of chemistry at MIT. He received a Ph. D. in physics from Columbia University in 1993, under the direction of Bruce Berne. After postdoctoral research with Greg Voth at University of Pennsylvania and with late Kent Wilson at UCSD, he jointed the MIT faculty in 1998. His research interests include statistical analysis of single molecule measurements, quantum dynamics of molecular systems, and self-assembly of colloids and polymers.

derived master equations using pathway summation.[11,12] Our self-consistent pathway solution differs because of the introduction of the self-consistency and applications to single molecule kinetics. Our results also support the analysis by Flomenbom and Silbey on the information content of on−off traces.[7] While they construct the canonical kinetic form from two-state trajectories, we arrive at the irreducible scheme by reducing an arbitrarily complex scheme with restrictions imposed by experimental detection and prior knowledge. The concept of the irreducible schemes can be related to a general definition of the information content of single molecule data, thus providing a basis for developing numerical analysis techniques.

The manuscript is arranged as follows: In section II, we introduce several single molecule quantities: first passage time distribution, interevent distribution, and event number distribution, present both the rate process formalism and waiting time distribution formalism, and then show their equivalence. In section III, we discuss two kinetic motifs, sequential reactions and branching reactions, which are the basic tools for decomposing and computing a complex kinetic scheme. As examples, we present self-consistent pathway solutions for two generic kinetics problems, enzymatic turnover in section IV and fluorescence emission in section V, and show a generic scheme composed of three basic links can describe both processes and their variations resulting from all possible combinations of subschemes. In section VI, we investigate the implication of our analysis for the interpretation of measurements in blinking experiments.

II. Single Molecule Measurements

We limit our discussions to renewal processes, where a single type of transitions is monitored, and refer readers to a future publication for discussions and references on nonrenewal processes (i.e., kinetic schemes with multiple types of monitored transitions).[8] Note that the definitions of renewal and nonrenewal processes depend on the detection scheme: If various types of transitions are detected separately, the single molecule measurement is a renewal process; otherwise, the measurement is a nonrenewal process. Thus, without multiple conformational channels, a complex chain reaction as described in section IV or a photon emission process in section V is a renewal process although the first passage time distribution is multiexponential and complicated. On the other hand, a simple decay process with two decay channels that are not detected separately is a nonrenewal process with memory effects. A renewal process with a single type of signal is completely specified by the distribution of the first passage time, $\phi(t)$, which is the probability distribution function of adjacent single molecule events, e.g., monitored enzymatic turnover events or detected photons. Depending on the type of kinetic processes, various terms have been associated with $\phi(t)$, including residence time, dwelling time, exit time, and turnover time. As shown below, once $\phi(t)$ is obtained, we can completely predict all other indicators of single molecule measurements. The key concept of our approach is to represent a complex kinetic scheme using waiting time distribution functions $Q(t)$. A first-order kinetic scheme is composed of fundamental rate steps, specified by rate constants k or equivalently by $Q(t) = ke^{-kt}$. But the waiting time distribution function can take an nonexponential form such as multiexponential, stretched exponential, and power-law decay. Thus, instead of the single rate constant associated with a fundamental rate step, $Q(t)$, can describe a distribution of rate constants, i.e., distributed rate processes. In this section, we formulate single molecule measurements with rate constants and with waiting time distribution functions, respectively, and then, in Appendix A, show their equivalence. We adopt the event-averaged initial condition in most of our calculations and briefly discuss the time-averaged initial condition in Appendix B. In Appendix C, we discuss an interesting relationship between the initial rise in the waiting time distribution and causal connectivity in kinetic networks.

A. Rate Formalism. For a single molecule scheme composed of exponential rate processes, the kinetics is completely specified by the rate matrix, $K_{ij} = \delta_{ij}k_j - (1 - \delta_{ij})k_{ij}$, where k_{ij} is the rate constant for the transition from state j to state i and $k_j = \Sigma_i k_{ij}$ is the depletion rate constant from state j. Then, the probability evolution, $P(t) = G(t)P(0)$, is governed by the Green's function, $G(t) = \exp(-Kt)$, or in Laplace space

$$G(s) = \frac{1}{sI + K} \tag{1}$$

where I is the identity matrix and the Laplace variable s denotes Laplace transforms. The rate matrix $K = K_D - K_{OD}$ is defined such that the diagonal elements K_D are positive and the off-diagonal elements–K_{OD} are negative. The Green's function $G(s)$ provides complete information on population dynamics in bulk, but the single molecule experiment probes additional information associated with the statistics of monitored events, e.g., emitted photons or enzymatic turnovers. The monitored transition from the jth state to ith state is described by $K' = k'_{ij}$, which is an off-diagonal element in the rate matrix K. Notice $k'_{ij} \neq k_{ij}$ since there can be multiple types of transitions from state j to i, and we assume only one type of transition is monitored. For example, the transition from the excited-state to the ground-state can occur through radiative decay, which is detected via emitted photons, or through nonradiative decay, which is not monitored. In the following, we consider four types of single molecule measurements illustrated in Figure 1 and the relevant transfer matrix expressions most closely related to these measurements.

Most of the expressions for rate processes have appeared in reviews on single molecule rate processes[13,14] and in standard literatures on renewal processes. Here, we include the rate formalism for completeness of our presentation and, more importantly, for the discussion on the equivalence between the two formalisms (see Appendix A).

1. A unique feature of single molecule measurements is the statistics and correlation of events along a single molecule trace. The key quantity is the PDF of the first passage time of the monitored transition, or equivalently, the distribution function

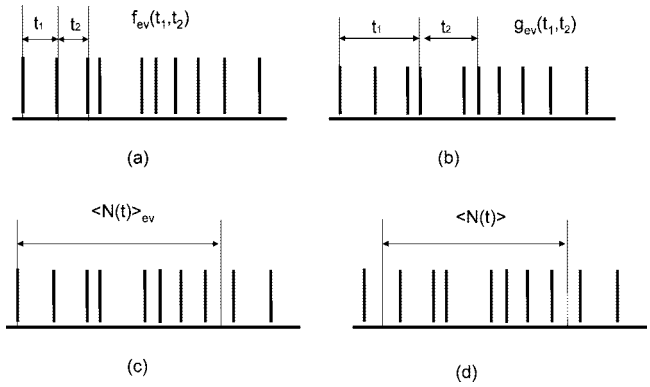

Figure 1. Schematic illustrations of the four measurements along a sequence of single molecule transition events: (a) the probability distribution function (PDF) of the first passage time, i.e., distribution of the adjacent transition events; (b) the PDF of two transition events regardless of the number of events in between, i.e., interevent distribution; (c) the event-averaged probability distribution of the number of events, i.e., intensity distribution; (d) the time-averaged probability distribution of the number of events.

between adjacent events, $\phi(t) = K'_{ij}G_{0,ji}(t)$, with the Green's function $G_0(t) = e^{-K_0 t}$. Here, the rate matrix K is separated into the monitored transition K' and the remaining part: $K = K_0 - K'$. In the Laplace domain, the PDF of the monitored events is

$$\phi(s) = K'_{ij}\left[\frac{1}{sI + K_0}\right]_{ji} = [K'G_0(s)]_{ii} \tag{2}$$

which is properly normalized as $\phi(s = 0) = 1$. Unless specified, indices i and j are associated with the monitored transition, and all other repeated indices in our expressions represent matrix multiplication and are summed over implicitly. As illustrated in Figure 1a, the PDF for observing a sequence of transitions is expressed as[15]

$$f_{m,ev}(t_1, t_2, \cdots, t_m) = [K'G_0(t_m - t_{m-1})K' \cdots G_0(t_2 - t_1) \times K'G_0(t_1)]_{ii} \tag{3}$$

where the event-averaged initial condition indicates the initial state for the time series, ith state. For nonrenewal processes, f_{ev} has been proposed as a direct measure for correlations between events, i.e., memory effects.[8,16] Often, we collect the number of monitored events, N, within a time window, t, as depicted in Figure 1c. Its nth moment is obtained from eq 3 as

$$\langle N(t)^n\rangle_{ev} = \sum_m m^n \left[\prod_{i=1}^{m}\int_{t_{i-1}}^{t} \mathrm{d}t_i\right]\sum_l [G_0(t - t_m) \times K' \cdots G_0(t_2 - t_1)K'G_0(t_1)]_{li} \tag{4}$$

where the integral variable t_i is time-ordered, the initial state is at the terminal state of the transition. The sum over the final state defines the survival probability, $S_i(t) = \Sigma_l[G_0(t)]_{li}$. Equation 4 can also be written in the Laplace form as

$$\mathcal{LT}\langle N(t)^n\rangle_{ev} = \sum_m m^n S_i(s)[K'G_0(s)]^m_{ii} \tag{5}$$

where $\mathcal{LT}$ denotes Laplace transformation.

2. The second type of single molecule measurements is the density and moment of monitored events, for example, the Poisson indicator and the renewal indicator. As depicted in Figure 1b, the direct route is to introduce $\psi(t)$, the PDF of observing another transition given the initial transition,[14,17]

$$\psi(s) = K'_{ij}\left[\frac{1}{sI + K}\right]_{ji} = [K'G(s)]_{ii} \tag{6}$$

which differs from eq 2 because of $K = K_0 - K'$. The asymptotic value of $\psi(t)$ is a constant given by the average mean passage time. Equation 6 is generalized to the multiple time number density

$$g_{m,ev}(t_1, t_2, \cdots, t_m) = [K'G(t_m - t_{m-1}) \cdots K'G(t_2 - t_1) \times K'G(t_1)]_{ii} \tag{7}$$

where $g_{ev}(t) = \psi(t)$ is also known as the photon correlation indicator often used in photon statistics (except for a constant prefactor). Once we have the number density, we can calculate the counting moments from[17]

$$C_{m,ev}(t) = \langle N(t)[N(t) - 1] \cdots [N(t) - m + 1]\rangle_{ev} = \prod_{i=1}^{m}\int_0^t \mathrm{d}t_i g_{m,ev}(t_1, t_2, \cdots, t_m) \tag{8}$$

which has a simple Laplace form

$$\mathcal{LT}[C_{m,ev}(t)] = \frac{m!}{s}[K'G(s)]^m_{ii} \tag{9}$$

with $m!$ arising from the multidimensional integral in eq 8.

3. The third type of single molecule measurements is the probability distribution for the number of observed events within a time bin, as shown in Figure 1c. The nth moments $\langle N(t)^n\rangle_{ev}$ are already given in terms of f_{ev} in eq 3 or g_{ev} in eq 7, which can be transformed to the probability distribution for $N(t)$, i.e., $P_{ev}(N, t) = \langle\delta(N(t) - N)\rangle_{ev}$. From eq 4 we identify this probability distribution

$$P_{ev}(N, t) = \prod_{i=1}^{N}\left[\int_{t_{i-1}}^{t} \mathrm{d}t_i\right]\sum_l [G_0(t - t_N)K' \cdots G_0(t_2 - t_1) \times K'G_0(t_1)]_{li} \tag{10}$$

A compact way to obtain the distribution and moments is the generating function method,[14,16,18] defined by

$$P_{ev}(z, s) = \mathcal{LT}\langle e^{izN(t)}\rangle = \sum_m S(s)[K'G_0(s)]^m_{ii}e^{izm} = \sum_l\left[\frac{1}{sI + K - e^{iz}K'}\right]_{li} \tag{11}$$

which is the Fourier transform of $P_{ev}(N, s)$. Explicitly, the event-averaged probability distribution of the number of events is given by

$$P_{ev}(N, s) = \frac{1}{2\pi}\int P_{ev}(z, s)e^{-izN}\,\mathrm{d}z \tag{12}$$

Taking derivatives with respect to z, we obtain the moments, $\langle N^n(t)\rangle_{ev}$, which is equivalent to eq 4.

4. As illustrated in Figure 1, the above three quantities are defined with the event-averaged initial condition specified with a monitored transition,[14,15] which can be acquired in single molecule experiments. An alternative approach is the time-averaged initial condition, where the initial time is randomly selected along the time axis, as shown in Figure 1d. Thus the probability of the first event is special and depends on the stationary distribution ρ as

$$\bar{\phi}(t) = \sum_l K'_{ij}G_{0,jl}(t)\rho_l \tag{13}$$

Here $K\rho = 0$ is stationary but not necessarily in equilibrium

unless the kinetic scheme satisfies detailed balance. Then, the probability for a sequence of events is

$$f_m(t_1, t_2, \cdots, t_m) = K' G_0(t_m - t_{m-1}) K' \cdots G_0(t_2 - t_1)\bar{\phi}(t_1) \tag{14}$$

which differs from eq 3 in the first event, and the probability distribution is given by

$$P(N, t) = \left[\prod_{i=1}^{N} \int_{t_{i-1}}^{t} \mathrm{d}t_i\right] S(t - t_N) K' \cdots G_0(t_2 - t_1)\bar{\phi}(t_1) \tag{15}$$

where the term $S(t) = \Sigma G_0(t)$ is the survival probability.

B. Waiting Time Distribution Formalism. We now discuss these experimental quantities in the language of waiting time distribution functions. To begin, we consider a general kinetic process, on a set of states $\{i\}$, with complex waiting time distribution functions, $Q(t) = \{Q_{ij}(t)\}$, where Q is the waiting time matrix and its matrix element Q_{ij} is the time-dependent transition probability from state j to state i. For rate processes discussed in section IIA, the waiting time distribution function for the monitored rate step is specified as $Q'_{ij}(t) = k'_{ij} \exp(-k_j t)$ or $Q'_{ij}(s) = k'_{ij}/(s+k_j)$, where $k_j = \Sigma_i k_{lj}$ is the depletion rate from the j state. Then, the probability evolution, $P(t) = G(t)P(0)$, is governed by the Green's function[10] given in Laplace space as

$$G(s) = S(s)\frac{1}{I - Q(s)} \tag{16}$$

where I is the identity matrix and the Laplace variable s denotes Laplace transforms. Here, the first term on the far right, $[I - Q(s)]_{ij}^{-1}$, is the probability of transition to the ith state given the initial state is j, and the term on the near right, $S_i(s) = [1 - \Sigma_l Q_{li}(s)]/s$, is the survival probability, i.e., the probability of not jumping out of the state i until time t.

1. The first type of single molecule measurements is the PDF of the first passage time of the monitored transition, or equivalently, the time distribution function between adjacent events, $\phi(t)$, which is given explicitly in Laplace space as

$$\phi(s) = Q'_{ij}(s)\left[\frac{1}{I - Q_0(s)}\right]_{ji} \tag{17}$$

where $Q_0 = Q - Q'$ is the waiting time distribution matrix, excluding the monitored transition. In Appendix B, eq 17 is shown to reduce to eq 2 for rate processes, indicating equivalence for all event-averaged quantities. As illustrated in Figure 1a, the PDF for observing a sequence of transition events is expressed as

$$f_{m,ev}(t_1, t_2, \cdots, t_m) = \phi(t_m - t_{m-1}) \cdots \phi(t_2 - t_1)\phi(t_1) \tag{18}$$

which can be used as a direct measure of correlations between events.[15,16] Then, the average moment of the monitored transitions is obtained from eq 18 as

$$\langle N(t)^n \rangle_{ev} = \sum_m m^n \left[\prod_{i=1}^{m} \int_{t_{i-1}}^{t} \mathrm{d}t_i\right] S(t - t_m) f_{m,ev}(t_1, t_2, \cdots, t_m) \tag{19}$$

where the integral variable t_i is time-ordered. $S(s) = [1 - \phi(s)]/s$ is the survival probability, the probability of not making a monitored transition. The moments can be written in the Laplace form as

$$\mathcal{LT}\langle N(t)^n \rangle_{ev} = \sum_m m^n S(s)\phi^m(s) \tag{20}$$

where $\mathcal{LT}$ denotes Laplace transformation. In Appendix A, the two forms of survival probability, $S(t)$, in eqs 19 and 4, are shown to be equivalent.

2. The second type of single molecule measurements is $\psi(t)$, the PDF of observing another transition given an initial transition at the initial time

$$\psi(s) = Q'_{ij}(s)\left[\frac{1}{I - Q(s)}\right]_{ji} \tag{21}$$

which differs from eq 17 because of $Q = Q_0 + Q'$. Equation 21 is generalized to the multiple time number density

$$g_{m,ev}(t_1, t_2, \cdots, t_m) = \psi(t_m - t_{m-1}) \cdots \psi(t_2 - t_1)\psi(t_1) \tag{22}$$

where $g_{ev}(t) = \psi(t)$ is the correlation indicator often used in photon statistics except for a constant prefactor. Using eq 22, we calculate the counting moments from[17]

$$C_{m,ev}(t) = \langle N(t)[N(t) - 1] \cdots [N(t) - m + 1] \rangle_{ev} = \prod_{i=1}^{m} \int_0^t \mathrm{d}t_i \, g_{m,ev}(t_1, t_2, \cdots, t_m) \tag{23}$$

which can also be expressed in a simple Laplace form

$$\mathcal{LT}[C_{m,ev}(t)] = \frac{m!\,\psi^m(s)}{s} \tag{24}$$

with $m!$ arising from the multidimensional integral in eq 23. The inter-event PDF, $\phi(s)$ in eq 17, and the PDF of adjacent events, $\psi(s)$ in eq 21, are related by

$$\psi(s) = \frac{\phi(s)}{1 - \phi(s)} \tag{25}$$

As demonstrated in Appendix A, this identity can also be confirmed for rate processes, using definitions in eq 6.

3. The third type of single molecule measurements is the probability distribution for the number of observed events within a time bin, which can be related to fluorescence intensity distribution. The nth moments $\langle N(t)^n \rangle_{ev}$ can be evaluated in terms of f_{ev} in eq 18 or g_{ev} in eq 22 and can be transformed to the probability distribution for $N(t)$, i.e., $P_{ev}(N, t) = \langle \delta(N(t) - N) \rangle_{ev}$. A convenient way to obtain this distribution is the generating function method,[14,16,18] defined as

$$P_{ev}(z, s) = \mathcal{LT}\langle \mathrm{e}^{izN(t)} \rangle = \sum S(s)\phi^m(s)\mathrm{e}^{izm} = \frac{1}{s}\frac{1 - \phi(s)}{1 - \mathrm{e}^{iz}\phi(s)} \tag{26}$$

which is the Fourier transform of $P(N, s)$. Taking derivatives with respect to z, we obtain the moments

$$\langle N^n(t) \rangle_{ev} = (-i)^n \left.\frac{\partial^n P_{ev}(z, t)}{\partial z^n}\right|_{z=0} \tag{27}$$

which is equivalent to eq 19 since we have used eq 20 in the derivation of eq 26. To show the equivalence between eqs 27 and 23, we construct a particular generating function of variable x using eq 25. The left-hand-side of eq 24 gives

$$\mathrm{LHS} = \sum \frac{\mathcal{LT}[C_m(t)]x^m}{m!} = \mathcal{LT}\langle (1 + x)^{N(t)} \rangle_{ev} \tag{28}$$

and the right-hand-side of eq 24 gives

$$\mathrm{RHS} = \frac{1}{s}\sum_m \psi^m(s)x^m = \frac{1}{s[1 - x\psi(s)]} \quad (29)$$

Changing the variable, $x = e^{iz} - 1$ and using eq 25 to replace $\psi(s)$ with $\phi(s)$, we recover exactly the generating function evaluated in eq 27, which yields the moment expressed by eq 26 or, equivalently, by eq 19. Thus we prove the equivalence of all three approaches for calculating moments $\langle N(t)^n\rangle_{ev}$.

4. Our discussion so far is limited to event-averaged single molecule quantities, which differ from time-averaged quantities in the selection of the initial counting time. As shown in Figure 1d, this initial time is selected randomly along the time axis in the time-averaged initial condition. Thus, the probability of the first counting event is proportional to the survival probability

$$\phi(t) = \frac{S(t)}{\langle t\rangle} \quad (30)$$

where $\langle t\rangle = \Sigma S(t)\, dt$ is the normalization factor. As a result, the PDF of a sequence is given by

$$f_m(t_1, t_2, \cdots, t_m) = \phi(t_m - t_{m-1}) \cdots \phi(t_2 - t_1)\phi(t_1) \quad (31)$$

which differs from eq 18 in the first event. In Appendix A, we show the equivalence between eqs 30 and 13, and therefore the equivalence for all time-averaged quantities. Several time-averaged quantities[13,19] including the Poisson indicator and the Mandel's Q parameter can be derived in a similar way and are discussed in Appendix B. A detailed calculation of the Poisson indicator and other time-averaged quantities are presented in section V for the example of single molecule photon statistics.

The waiting time distribution formalism discussed here is the starting point of self-consistent pathway analysis in this article. The rate matrix formalism in section IIA is standard for single molecule kinetics, which is first order by definition. As shown in Appendix B, the rate formalism and waiting time distribution formalism are completely equivalent. The equivalence is expected, as exponential rate processes are a special case of general waiting time distribution processes and the complex waiting time distribution processes can always be decomposed into a set of first-order rate processes.

In the single molecule community, various terms have been used for measured time intervals, including waiting times, dwelling times, first passage times, first arrival times, and survival times. The complete information of a renewal process is contained in the distribution of the first passage time $\phi(t)$, but the interpretation of the underlying kinetics responsible for $\phi(t)$ is not unique. Nevertheless, one can relate the short time rise of $\phi(t)$ to the causal connectivity of chemical reactions (see Appendix C for details). Furthermore, we recently established a signature of detailed balance violation: If $\phi(t)$ does not decay monotonically, the probed kinetics must be a part of underlying kinetic loop(s) that supports a nonequilibrium flux.[20] Thus nonmonotonic decay in $\phi(t)$ introduces an additional restriction to the underlying rate process.

The discussion in this article is limited to renewal processes with a single type of monitored events and will be extended to nonrenewal processes in a future publication.[8] For experiments with one type of monitored measurement (e.g., enzymatic turnover or photon emission), the PDF of the first passage time, $\phi(s)$, completely specifies single molecule data in a renewal process. In comparison, a set of PDFs are needed to specify single molecule data in a nonrenewal process, thus causing correlation between events, i.e., the memory effects. The definitions in this section and the analysis that follows can be generalized using tensor notations to describe nonrenewal processes with multiple emission states and multiple conformation channels. The order of variables in eqs 16−23 is irrelevant for renewal processes, but becomes important in the generalization to nonrenewal processes.

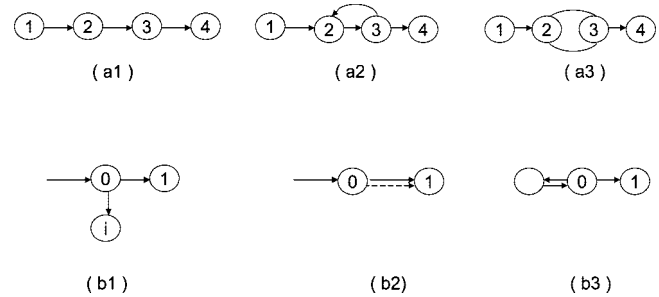

Figure 2. Examples of sequential motif (a) and branching motif (b): (a1) a sequential reaction with three irreversible steps, (a2) a sequential reaction with a reversible intermediate step, (a3) a sequential reaction where the intermediate step is a complex subscheme, (b1) a branching reaction with decay to different states, (b2) a branching reaction with two different decay channels to the same final state, and (b3) a branching reaction with one of the decay channels back to the reactant state.

Evidently, the various types of measurements are essentially equivalent for renewal processes and can be related to each other. The choice of approach is a matter of convenience and conceptual simplicity. In the article, we will focus on the calculation of $\phi(t)$, which is the basic quantity for evaluating all measurements discussed above.

III. Kinetic Motifs

A kinetic scheme can be characterized by a kinetic motif or a set of kinetic motifs, which are salient features in the connectivity of states.[9] The basic kinetic motifs are sequential and branching, as illustrated in Figure 2. In sequential kinetics, a set of states are arranged in a linear and irreversible configuration. The distribution function for the overall waiting time in Figure 2(a1)–(a3) is

$$\prod Q(s) = Q_{43}(s)\tilde{Q}_{32}(s)Q_{21}(s) \quad (32)$$

where $\tilde{Q}$ represents the possible summation of intermediate reaction pathways within a subscheme. Since it takes finite time for the system to pass through two or more sequential links, the PDF of jumping from the first to final state instantaneously is zero and will reach a peak on an intermediate time-scale. The intermediate kinetics can be a simple irreversible step as indicated in Figure 2,a1, $\tilde{Q}_{32}(s) = Q_{32}(s)$, a reversible step as in Figure 2,a2, $\tilde{Q}_{32}(s) = [1 - Q_{32}(s)Q_{23}(s)]^{-1}Q_{32}(s)$, and an arbitrarily complex subscheme as Figure 2,a3. As long as the first and last transitions are irreversible and none of the transitions in between is monitored, the overall kinetics from the initial to final states can be concatenated into a single waiting time distribution $\tilde{Q}$. This procedure helps us to reduce a complex reaction scheme into a scheme of minimal complexity, i.e., the generic kinetic scheme.

The second motif is branching, through which a state can decay via several channels to different states as in Figure 2,b1, to the same states as in Figure 2,b2, or back to the original state as in Figure 2,b3. In all these cases, we can write the waiting time distribution for the decay as

$$\sum_i Q_{i0}(t) = Q_{10}(t) + Q_{20}(t) + \ldots \quad (33)$$

where 0 denotes the original state from which population depletes. A good example of branching kinetics is triplet

blinking, where the excited system can decay through fluorescence or can be trapped in the triplet state. If the decay rate from the triplet state is sufficiently slow, the system becomes dark for a long period of time. The alternating dark and bright periods lead to triplet blinking and effectively cause photon bunching. More discussion on triplet blinking is presented in section V. To relate to underlying mechanisms, we need to examine the effect of branching on the definition of $Q_{i0}(t)$ for ith decay channel. The overall survival probability of the initial state is $S(t) = \Pi S_i(t)$, where $S_i(t)$ is the survival probability with only the ith channel present and $Q_i(t) = -\dot{S}_i(t)$ is the corresponding waiting time distribution function. Then, we have the explicit expression for multiple channel decay

$$\sum_i Q_{i0}(t) = -\dot{S}(t) = \sum_i Q_i(t) \prod_{j \neq i} S_j(t) \tag{34}$$

from which the PDF of decaying through the ith channel is identified as $Q_{i0}(t) = Q_i(t)\Pi_{j\neq i}S_j(t)$. Together, eqs 32 and 33 along with eq 34 allow us to derive explicit expressions for the distribution of the first passage time for a complex scheme.

IV. Example I: Michaelis−Menten Mechanism

Our first example is motivated by the enzymatic turnover reaction with possible extension to molecular motors. As shown in the basic scheme for enzymatic reactions in Figure 3a, starting from state 1, a substrate [S] binds with the enzyme [E] to form a substrate-enzyme complex [ES], i.e., state 2, which can branch to form a product [P] or return to the state 1. Using eqs 32 and 33, the distribution of turnover time is found to satisfy the self-consistent equation

$$\phi(s) = [Q_{32}(s) + \phi(s)Q_{12}(s)]Q_{21}(s) \tag{35}$$

where the two terms in the bracket represent the branching at the [ES] state. Solution to eq 35 yields

$$\phi(s) = Q_{32}(s)\frac{1}{1 - Q_{21}(s)Q_{12}(s)}Q_{21}(s) = Q_{32}(s)\tilde{Q}_{21}(s) \tag{36}$$

where $\tilde{Q}_{21}(s)$ represents the reversible process from the initial state 1 to the intermediate state 2 (a simple kinetic loop). In eq 36, $Q_{32}(s)$ describes the monitored transition, $Q_{21}(s)$ describes the controlled transition which depends on the substrate concentration [S], and $\phi(s)$ describes single enzymatic turnover measurements.

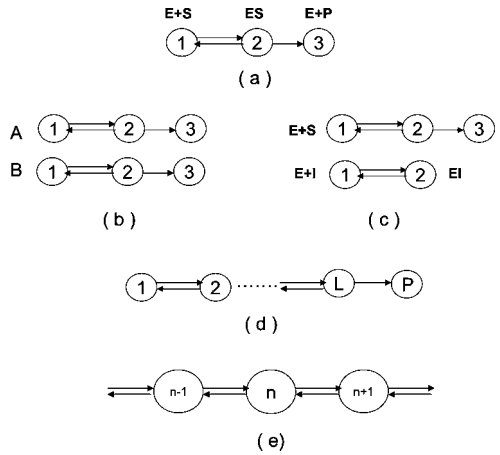

Figure 3. Models of reversible chain reactions: (a) the generic scheme of enzymatic turn-over reactions; (b) an enzymatic reaction with two competing substrates, A and B; (c) an enzymatic reaction with the possibility of deactivation due to binding with inhibitors; (d) an enzymatic reaction with a sequence of conformational transitions; and (e) a molecular motor on a one-dimensional lattice.

The average passage time of the turnover reactions can be calculated from eq 36, assuming $Q_{21}(s) = 1 - s\tau_1 + ...$, $Q_{12}(s) = (1 - q)(1 - s\tau_2 + ...)$, and $Q_{32}(s) = q(1 - s\tau_2 + ...)$, where q is the branching ratio between two decay channels from state 2, τ_2 is the average lifetime at state 2, and τ_1 is the average lifetime at state 1. Taking the derivative of eq 36, $\tau = -\partial\phi(s = 0)/\partial s$, we obtain the average turnover rate

$$\langle t \rangle = \frac{\tau_1 + \tau_2}{q} \tag{37}$$

which is identical to Ninio's pathway derivation of the first passage time. For a rate process, we assign $1/\tau_1 = k_1 = k_1^0[\mathrm{S}]$, $1/\tau_2 = k_{-1} + k_2$, and $q = k_2/(k_2 + k_{-1})$, where [S] is the substrate concentration, k_1^0 is the substrate binding constant, and k_2 is the catalytic rate. Then, we recover the Michaelis−Menten expression[21−23]

$$k = \frac{1}{\langle t \rangle} = \frac{k_2 k_1^0[\mathrm{S}]}{k_2 + k_{-1} + k_1^0[\mathrm{S}]} = \frac{k_2[\mathrm{S}]}{K_\mathrm{M} + [\mathrm{S}]} \tag{38}$$

where $K_\mathrm{M} = (k_2 + k_{-1})/k_1^0$ is the Michaelis constant. The Michaelis−Menten expression in eq 38 is a special case of eq 37, which is not limited to rate processes. All above expressions can be obtained by solving the transfer matrix solution in eq 17 with $Q'(s) = Q_{32}(s)$, but, as will be seen below, the self-consistent pathway solution is generic for a class of problems and provides more insights.

A. Substrate Selectivity and Inhibition. An interesting extension of the Michaelis−Menten mechanism is the competition of two substrates with an enzyme and the inhibitor-induced suppression of catalytic turnovers. As shown in Figure 3b, the enzyme binds with a substrate, either [S_A] or [S_B], to form the substrate−enzyme complexes [ES_A] or [ES_B], which can dissociate and restart the process, or decay to the product. In analogy to the derivation of eq 35, the overall distribution function for the turnover time, obeys the self-consistent equation

$$\phi(s) = [Q_{\mathrm{A},32}(s) + \phi(s)Q_{\mathrm{A},12}(s)]Q_{\mathrm{A},21}(s) + [Q_{\mathrm{B},32}(s) + \phi(s)Q_{\mathrm{B},12}(s)]Q_{\mathrm{B},21}(s) \tag{39}$$

where the subscripts A and B denote the two reactions associated with the two substrates. Solution to eq 39 yields

$$\phi(s) = \frac{Q_{\mathrm{A},32}(s)Q_{\mathrm{A},21}(s) + Q_{\mathrm{B},32}(s)Q_{\mathrm{B},21}(s)}{1 - Q_{\mathrm{A},21}(s)Q_{\mathrm{A},12}(s) - Q_{\mathrm{B},21}(s)Q_{\mathrm{B},12}(s)} = Q_{\mathrm{A},32}(s)\tilde{Q}_{\mathrm{A},21}(s) + Q_{\mathrm{B},32}(s)\tilde{Q}_{\mathrm{B},21}(s) \tag{40}$$

where the first term is the turnover time distribution for substrate A, $\phi_\mathrm{A}(s) = Q_{\mathrm{A},32}(s)\tilde{Q}_{\mathrm{A},21}(s)$, and the second term is the turnover time distribution for substrate B, $\phi_\mathrm{B}(s) = Q_{\mathrm{B},32}(s)\tilde{Q}_{\mathrm{B},21}(s)$. The enzyme specificity is defined as the ratio of turnover velocities and is given by

$$\frac{v_\mathrm{A}}{v_\mathrm{B}} = \frac{\phi_\mathrm{A}(s=0)}{\phi_\mathrm{B}(s=0)} = \frac{p_\mathrm{A}q_\mathrm{A}}{p_\mathrm{B}q_\mathrm{B}} \tag{41}$$

where $p_\mathrm{A} = Q_{\mathrm{A},21}(s = 0)$ and $p_\mathrm{B} = Q_{\mathrm{B},21}(s = 0)$ are the probabilities for an enzyme to bind with two types of substrates and $q_\mathrm{A} = Q_{\mathrm{A},32}(s = 0)$ and $q_\mathrm{B} = Q_{\mathrm{B},32}(s = 0)$ are the branching probabilities for the two substrates, respectively. For a rate process, we assign $p_\mathrm{A}/p_\mathrm{B} = k_{\mathrm{A},1}^0[\mathrm{S_A}]/k_{B,1}^0[\mathrm{S_B}]$, $q_\mathrm{A} = k_{\mathrm{A},2}/(k_{\mathrm{A},2} + k_{\mathrm{A},-1})$, and $q_\mathrm{B} = k_{\mathrm{B},2}/(k_{\mathrm{B},2} + k_{\mathrm{B},-1})$. Then, we recover the

standard result for enzyme specificity

$$\frac{v_A}{v_B} = \frac{[S_A]k_{A,2}/K_{A,M}}{[S_B]k_{B,2}/K_{B,M}} \tag{42}$$

which is a special case of the more general expression in eq 41.

A simple extension of eq 39 is the suppression of enzymatic activity by an inhibitor, as illustrated in Figure 3c, which can be treated as a special case of the scheme in Figure 3b, when one of the substrates can bind but cannot react. With the nonreactive inhibitor, the self-consistent solution in eq 40 becomes

$$\phi(s) = \frac{Q_{S,32}(s)Q_{S,21}(s)}{1 - Q_{S,21}(s)Q_{S,12}(s) - Q_{I,21}(s)Q_{I,12}(s)} \tag{43}$$

where the subscript S represents the substrate and the subscript I represents the inhibitor. To proceed, we assume the general form for the waiting time distribution: $Q_{S,21}(s) = p(1 - s\tau_1 + ...)$, $Q_{S,12}(s) = (1 - q)(1 - s\tau_2 + ...)$, $Q_{S,32}(s) = q(1 - s\tau_2 + ...)$ for reactions with the substrate, and $Q_{I,21}(s) = (1 - p)(1 - s\tau_1 + ...)$, $Q_{I,12}(s) = (1 - s\tau_{I,2} + ...)$ for the deactivation due to binding with the inhibitor. Here, p is the probability of binding with substrates and $(1 - p)$ is the probability of binding with inhibitors. Then, the average lifetime evaluated from $\phi(s)$ is

$$\langle t \rangle = \phi(s=0) = \frac{1}{pq}[\tau_1 + p\tau_2 + (1-p)\tau_{I,2}] \tag{44}$$

which reduces to eq 37 in the limit of $p = 1$. For a rate process, we can use the rate constants to define $p = k_1^0[S]/(k_1^0[S] + k_{1,1}^0[I])$, $\tau_1 = 1/(k_1^0[S] + k_{1,1}^0[I])$, $\tau_2 = 1/(k_{-1} + k_2)$, $q = k_2/(k_{-1} + k_2)$, and $\tau_{I,2} = 1/k_{I,-1}$. As a result, we obtain the rate expression

$$k = \frac{1}{\langle t \rangle} = \frac{k_2[S]}{[S] + K_M\left(1 + \frac{k_{I,1}}{k_{I,-1}}[I]\right)} \tag{45}$$

where the bracket term represents the competition due to the inhibitor-enzyme binding.

B. Chain Reactions. The basic Michaelis−Menten mechanism is the generic reaction scheme for enzymatic reactions and can be extended to a chain of conformational changes[21] as illustrated in Figure 3d. Let us denote the PDF of the first passage time starting from the n-th conformation to the final product as $\phi_n(s)$. Then, we use the concept of branching to construct the self-consistent relation

$$\phi_n(s) = \phi_{n+1}(s)Q_{n+1,n}(s) + \phi_{n-1}(s)Q_{n-1,n}(s) \tag{46}$$

which is supplemented with the boundary conditions, $\phi_1(s) = \phi_2(s)Q_{21}(s)$ and $\phi_L(s) = Q_{L+1,L}(s)$ with $L + 1$ denoting the product state. Starting from $\phi_1(s)$, the self-consistent pathway equation, eq 46, can be solved iteratively, giving

$$\phi_2(s) = \phi_3(s)Q_{32}(s)\frac{1}{1 - Q_{21}(s)Q_{12^{(s)}}} = \phi_3(s)\tilde{Q}_{32}(s)$$

$$\phi_3(s) = \phi_4(s)Q_{43}(s)\frac{1}{1 - \tilde{Q}_{32}(s)Q_{23^{(s)}}} = \phi_4(s)\tilde{Q}_{43}(s) \tag{47}$$

which is closed at the final state with the terminal boundary condition at $n = L$. In eq 47, $\tilde{Q}_{n+1,n}$ represents the contribution from all the states to the left of the nth state in Figure 3d, which is a subscheme of the chain reaction. Interestingly, the iterative solution eq 49 takes a generalized Michaelis−Menten form as in eq 38 but with a redefined PDF $\tilde{Q}$.

To obtain an explicit expression for the rate constant, we assume the general form for the waiting time distribution functions $Q_{n+1,n}(s) = q_n(1 - s\tau_n + ...)$ and $Q_{n-1,n}(s) = (1 - q_n)(1 - s\tau_n + ...)$, where q_n is the branching ratio at state n and τ_n is the lifetime at state n. Taking derivative of eq 46 with respect to Laplace variable s, we obtain

$$\langle t_n \rangle = \langle t_{n+1} \rangle q_n + \langle t_{n-1} \rangle (1 - q_n) + \tau_n \tag{48}$$

with the boundary condition $q_1 = 1$ and $\langle t \rangle_{L+1} = 0$. Solving the above equation iteratively, we arrive at an explicit expression for the average turnover rate

$$\langle t \rangle = \sum_{n=1}^{L}\sum_{i=1}^{n-1}\frac{\tau_i}{q_i}\prod_{j=i+1}^{n}\left(\frac{1}{q_j} - 1\right) + \sum_{n=1}^{L}\frac{\tau_n}{q_n} \tag{49}$$

which is derived in Appendix D. Similar results for chain reactions have been obtained in the literature using other methods.[11,24] As expected, as long as the first step $Q_{21}(s)$ is characterized by a rate constant proportional to [S], $\tau_1 \propto 1/[S]$, the overall rate will take the functional form of the Michaelis−Menten expression in eq 37, although the definitions for k_2 and k_{-1} will depend on the details of subsequent reactions in Figure 3d.

The chain reaction can be further extended to an infinite one-dimensional lattice, as shown in Figure 3e, which is a basic model for molecular motors. Introducing the translational invariance with repeated units and proper boundary conditions, one can solve eq 46 self-consistently and give the velocity and diffusion constant of a molecular motor along the one-dimensional lattice.[25−27]

V. Example II: Fluorescence Emission

The second example models room-temperature fluorescent emission from a molecular system with ground, excited, triplet, and fluorescent emission states.[13,28−30] As shown in Figure 4, the complete kinetic scheme consists of the excitation from the ground-state to the excited state, Q_{exc}; relaxation from the excited-state to the fluorescent emission state, Q_{rel}; intersystem crossing from the fluorescent state to the triplet state, Q_{isc}; decay from the triplet state to the ground state, Q_t; all other nonra-

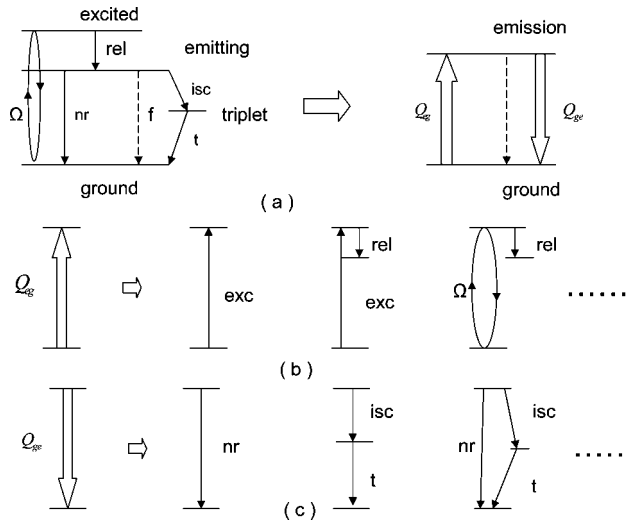

Figure 4. Kinetic models for fluorescence emission: (a) reduction of the emission scheme on the left to the generic irreducible scheme on the right, (b) possible subschemes associated with the excitation transition, and (c) possible subschemes associated with nonradiative decay.

diative decay from the emission state, Q_{nr}; and spontaneous fluorescent photon emission, Q_f.[31,32] Using the principle illustrated in Figure 2c, we can denote all kinetic routes from the ground to the fluorescent state as Q_{eg}, all kinetic routes from the fluorescent state to the ground state, except for fluorescent decay, as Q_{ge}, and the fluorescent decay as Q'_{ge}. Then, the complex scheme reduces the irreducible generic scheme in Figure 4a, which is the minimal scheme to represent a more complex kinetics scheme, but the maximal scheme to define the information content of fluorescence emission experiments. Interestingly, the irreducible generic scheme in Figure 4a is essentially the same as Figure 3a, although the physical processes and measured quantities are different.

We now calculate the first passage time distribution for detecting photons, $\phi(t)$, in the irreducible generic model. Starting from the ground state, the system makes a transition to the fluorescent state and then branches to the fluorescent channel and the nonfluorescent channel. In the latter case, the system returns to the ground-state without emitting a photon and restarts the above renewal process. Following the reaction pathways, we have the self-consistent equation

$$\phi(s) = [\phi(s)Q_{ge}(s) + Q'_{ge}(s)]Q_{eg}(s) \tag{50}$$

which is solved to yield

$$\phi(s) = Q'_{ge}(s)\frac{1}{1 - Q_{eg}(s)Q_{ge}(s)}Q_{eg}(s) = Q'_{ge}(s)\tilde{Q}_{eg}(s) \tag{51}$$

where $\tilde{Q}_{eg}(s)$ represents all possible transitions from the ground-state to the emission state without fluorescence. As expected, eqs 51 and 36 share the same functional form since both processes have three basic transitions and the simple generic scheme. In Figure 4a, $Q'_{ge}(s)$ is the monitored transition, $Q_{eg}(s)$ is the controlled transition, and $Q_{ge}(s)$ is the hidden transition. By means of eq 51, the measurement of $\phi(s)$ leads to the determination of the waiting time distribution $Q_{ge}(s)$, which defines the maximal amount of information from single molecule time series provided prior knowledge about the excitation process and fluorescence emission process.

The complex waiting time distribution Q_{eg} in Figure 4b can be a direct excitation, $Q_{eg}(s) = Q_{exc}(s)$, an excitation convoluted with relaxation, $Q_{eg}(s) = Q_{rel}(s)Q_{exc}(s)$, or a two-level quantum transition. The case of the quantum two-level system in Figure 4b has been studied intensively and can be solved on the basis of the optical Bloch equation, which takes the form of 4-state kinetics with two virtual states associated with quantum coherence. The complex waiting time distribution Q_{ge} in Figure 3c, can be a simple nonradiative decay $Q_{ge}(s) = Q_{nr}(s)$, transfer through the intermediate triplet state $Q_{ge}(s) = Q_{isc}(s)Q_t(s)$, or transfer through both the triplet state and other nonradiative channels $Q_{ge}(s) = Q_{nr}(s) + Q_{isc}(s)Q_t(s)$. Plugging these expressions into eq 51, we get a formal expression for the photon waiting time distribution $\phi(s)$ and thus all of the single molecule measurements.

As shown above, eq 51 provides a complete theoretical description of single molecule photon emission processes. However, the application of eq 51 to real experiments can be complicated by experimental details, such as background noise and detector dark periods. With suitable models, we can incorporate these realistic considerations into $Q(s)$ and hence apply our generic scheme in Figure 4 to the analysis of real experiments.

General expressions can also be derived with the three waiting time distribution functions expanded to second moments as $Q_{eg}(s) = (1 - s\tau_{eg} + s^2\eta_{eg} + ...)$, $Q_{ge}(s) = (1 - q)(1 - s\tau_{ge} + s^2\eta_{ge} + ...)$, and $Q'_{ge}(s) = q(1 - s\tau'_{eg} + s^2\eta'_{eg} + ...)$, where τ is the average waiting time for each transition and η is the second moment of the waiting time defined as $\eta = 2\int Q(t)t^2\,dt$. Then, using eq 51, we obtain the average interphoton distance

$$\langle t \rangle = \frac{\tau_{eg} + (1 - q)\tau_{ge} + q\tau'_{ge}}{q} \tag{52}$$

and the Mandel's $\mathcal{Q}$ parameter

$$\mathcal{Q}_M = \frac{1}{\langle t \rangle^2}\left[(\tau'_{ge}\tau_{eg} + \eta'_{ge}) + \frac{1}{q}\eta_{eg} + \frac{1 - q}{q}(\tau_{ge}\tau_{eg} + \eta_{ge})\right] - \frac{1}{\langle t \rangle}[\tau'_{ge} + \tau_{eg}] \tag{53}$$

Assuming a Gaussian distribution, we can use the above two expressions to evaluate $P(N, t)$ as shown in Appendix B. The same results for $\langle t \rangle$ and $\mathcal{Q}_M$ can also be obtained from the interevent PDF

$$\psi(s) = \frac{Q_{eg}Q'_{ge}}{1 - Q_{eg}[Q_{ge} + Q'_{ge}]} \tag{54}$$

using $\psi(s) = 1/s\langle t \rangle + \mathcal{Q}_M/2$. For all possible combinations of Q_{eg} and Q_{ge} in Figure 4, we simply substitute the relevant waiting time distribution function Q's, or corresponding τ's and η's, into eqs 51−54 to find analytical expressions for photon counting quantities. Here we discuss coherent excitations and triplet blinking to demonstrate the generality of our expressions for $\phi(t)$, $\psi(t)$, $\langle t \rangle$, and $\mathcal{Q}_M$ in terms of the three waiting time PDF's.

A. Coherent Excitation. Photon statistics of driven two-level systems is a well-studied problem in quantum optics. For simplicity of presentation, we will not include the explicit solution but refer readers to standard textbooks and review articles. Here, we discuss the relevance of quantum coherence in our generic scheme analysis and explore quantum effects not included in the optical Bloch equation.

• Since spontaneous emission is an incoherent classical decay, the statistics of fluorescence photons is a standard chemical kinetics problem, where quantum coherence is destroyed whenever a photon is emitted. The spontaneous emission process is completely captured by the waiting time distribution function $Q_{eg}(s)$. The situation is quite different if absorption, stimulated emission, and multidimensional spectroscopy[33] is measured, because such quantum processes cannot be treated directly as a simple kinetics problem.[17]

• A particularly simple example is fluorescence emission from driven two-level systems. With some approximations, the simplest description of the system is the optical Bloch equation, which defines a rate process for the density matrix or, effectively, a four-state classical kinetics problem.[13,33,34] Since the fluorescent measurement is related to the population at the emission state, the diagonal matrix elements define two virtual states associated with quantum coherence and can be incorporated into $Q_{eg}(s)$ as intermediate states. In fact, photon statistics associated with the optical Bloch equation is a standard problem, and the resulting photon density correlation and Mandel's $\mathcal{Q}$ parameter are given in the literature.[35] The same argument also applies to three-level systems, four-level systems, or generally, N-level systems. Absorption and simulated emission are not treated as simple classical kinetics because the processes are associated with off-diagonal matrix elements.

• Typical time-scales of dissipative environments in condensed phase systems are not necessarily short enough to justify the use of the Markovian approximation assumed in the optical

Bloch equation. Many non-Markovian solutions are available and can be generally considered as rate problems with higher-order density matrices, e.g., $\{\rho_e, \rho_{eg}, \rho_{eeg}, ...\}$. Thus, our approach remains applicable for non-Markovian dissipation with a complex effective waiting time distribution function.

• Photon statistics have been computed recently for model systems with the optical Bloch equation, but the implicit approximations may cause difficulties in several situations, including non-Markovian dissipation. For example, strong electric fields and low temperatures may prevent the use of the optical Bloch equation and will require more careful treatments of quantum coherence and dissipation.

B. Triplet Blinking. As an example, we consider a three-state scheme[13,28−30] composed of a direct excitation, i.e., the first possible subscheme in Figure 4b, the nonradiative relaxation with the presence of a triplet state, i.e., the third possible subscheme in Figure 4, and radiative decay. The focus of the calculation is mainly on $Q_{ge}(s)$, which involves the triplet state and nonradiative channel. To simplify the calculation, we assign the waiting time PDF's with rate constants, giving $Q_{eg}(s) = k_{exc}/(s + k_{exc})$, $Q'_{ge}(s) = k_f/(s + k_f + k_{isc} + k_{nr})$, and

$$Q_{ge}(s) = \frac{k_{nr} + k_{isc}k_t/(s + k_t)}{s + k_{nr} + k_{isc} + k_f} \tag{55}$$

with the fluorescence rate k_f, excitation rate k_{exc}, nonradiative relaxation rate k_{nr}, intersystem crossing rate k_{isc}, and triplet state relaxation rate k_t. Substituting these waiting time PDF's for rate processes into eqs 51 and 54, we have the distribution of adjacent photons

$$\phi(s) = \frac{k_f k_{exc}(s + k_t)}{(s + k_{exc})(s + k_t)(s + k_f + k_{nr} + k_{isc}) - k_{exc}[k_{nr}(s + k_t) + k_t k_{isc}]} \tag{56}$$

and the interphoton distribution

$$\psi(s) = \frac{\phi(s)}{1 - \phi(s)} = \frac{k_f k_{exc}(s + k_t)}{s[(s + k_t)(s + k_f + k_{nr} + k_{isc}) + k_{exc}(s + k_t + k_{isc})]} \tag{57}$$

Comparing second-order expansion of Q's, we can identify τ and η and then use eqs 52 and 53 to find the inverse of average first passage time or the average fluorescent rate

$$k = \frac{1}{\langle t \rangle} = \frac{k_f k_{exc} k_t}{k_t(k_{nr} + k_{isc} + k_f) + k_{exc}(k_{isc} + k_t)} \tag{58}$$

and the Mandel's $\mathcal{Q}$ parameter

$$\mathcal{Q}_M = \frac{2k_f k_t(k_{isc}k_{exc} - k_t^2)}{[k_t(k_{nr} + k_{isc} + k_f) + k_{exc}(k_{isc} + k_t)]^2} \tag{59}$$

The results have been obtained earlier by solving rate equations[13,29] and are presented here as a special case of our general solutions in eqs 51−54.

The complicated expressions can be simplified to two limiting cases. For $k_{isc}k_{exc} < k_t^2$, the decay from the triplet state is sufficiently fast and the original reaction scheme reduces to scheme 1 of Figure 5, which explains the antibunching mechanism. The reduced scheme yields $k = k_f k_{exc}/(k_{nr} + k_{isc} + k_f + k_{exc})$ and $\mathcal{Q}_M = -2k_f k_t/(k_{isc} + k_{nr} + k_f + k_{exc})$, which are consistent with eq 57 as $k_t \to \infty$. For $k_{isc}k_{exc} > k_t^2$, the decay rate from the triplet state is sufficiently slow so that the system can be trapped and becomes dark. The alternating dark and bright periods lead to triplet blinking, effectively causing photon bunching. The original reaction scheme reduces to scheme 2 of Figure 5, where the branching rate to the triplet state is

$$\gamma = k_{isc}k_{exc}/(k_{exc} + k_{isc} + k_{nr} + k_f) \tag{60}$$

The reduced scheme yields $k = k_f k_t/k_{isc}$ and $Q_M = 2k_f k_t/(k_{exc}k_{isc})$, which are consistent with eq 57 as $k_t \to 0$. From these two limiting cases, we conclude that the sign of Q_M in a renewal process reflects the competition of the two basic motifs: antibunching caused by sequential kinetics and bunching caused by branching kinetics.

C. Average Photon Counting Quantities. The average fluorescence intensity is inversely proportional to the average passage time, $\bar{I} \propto 1/\langle t \rangle$. If the triplet lifetime τ_t is long, eq 52 is dominated by the second term in the numerator, giving

$$\bar{I} \propto \frac{1}{\langle t \rangle} \approx \frac{q}{(1 - q)\tau_t} \tag{61}$$

For the usual rate process, the branching ratio is given by $q = k_t\tau'_{ge}$. which is the quantum yield in the context of fluorescence detection, i.e.

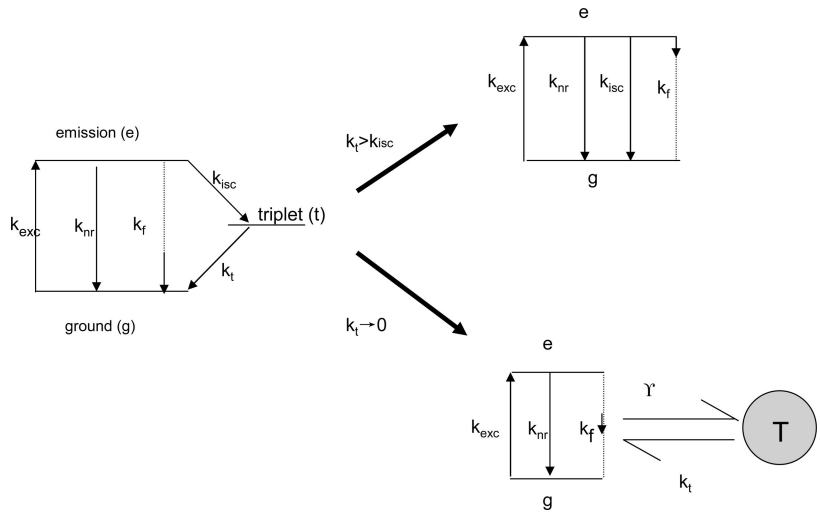

Figure 5. Three-state system consisting of ground, singlet, and triplet states. If the triplet relaxation rate is fast, the three-state model reduces to scheme 1, an effective two-state model; if the triplet relaxation rate is slow, the three-state model reduces to scheme 2, which is responsible for triplet blinking. In scheme 2, the branching rate γ is defined in text.

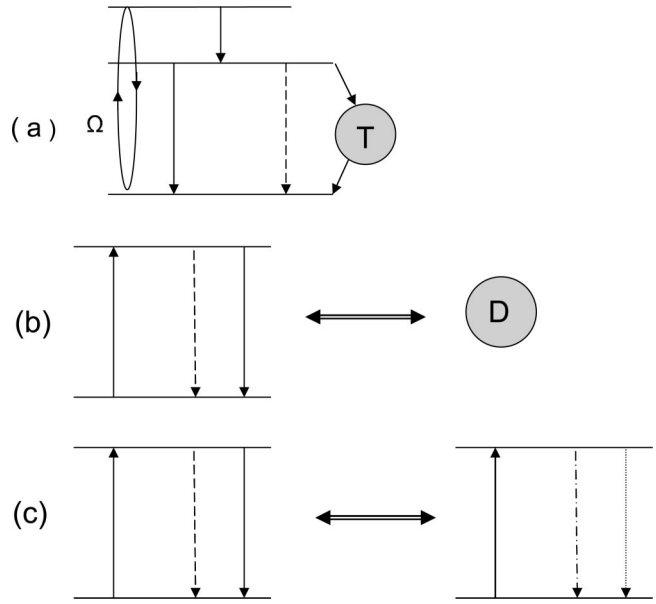

Figure 6. Possible generic schemes of quantum dots emission kinetics: (a) single emission state, (b) one bright and one dark state, and (c) modulated multiple emission states.

$$q = \frac{Q'_{ge}(s=0)}{Q'_{ge}(s=0) + Q_{ge}(s=0)} = \frac{k_f}{k_f + k_{nr} + k_{isc}} \quad (62)$$

The fluorescent lifetime distribution is given by $Q'_{ge}(t)$ as

$$f(t) = \frac{Q'_{ge}(t)}{\int Q'_{ge}(t)\,dt} = (k_f + k_{nr} + k_{isc}) \exp[-(k_f + k_{nr} + k_{isc})t] \quad (63)$$

where the denominator is the branching ratio. It should be noted that $Q'_{ge}(t)$ depends not only on fluorescence decay but also on nonradiative decay. According to eq 34, the observed lifetime is the sum of all decay channels, giving

$$k_{obs} = k_f + k_{nr} + k_{isc} = k_f/q \quad (64)$$

If the quantum yield is large, i.e., $q \to 1$, then radiative decay dominates and the observed lifetime is approximately the fluorescence lifetime, $k_{obs} \approx k_f$. Our results here are limited to the experimental setup of continuous illumination and, with some modifications, can be extended to other experimental set-ups.[30,36,37]

VI. Nonexponential Waiting Time Distributions and Generic Schemes for Single Molecule Blinking

To understand the underlying physical mechanisms for the nonexponential waiting time distribution, $Q(t)$, we now discuss several scenarios of dynamic and static disorder and their implications for the measurements of blinking phenomena.

1. In the first scenario, the single molecule system selects a new rate constant from a rate distribution $\rho(k)$ for every transition event, each transition event is exponentially distributed, and an average over many events along the trace yields the nonexponential decay $Q(t) = \int \rho(k)\, e\exp(-kt)\, dk$. $Q(t)$ thus defined decays monotonically, $\partial^n Q(t)/\partial t^n > 0$, imposing a constraint on the experimentally observed waiting distribution function. Single molecule measurements associated with this type of disorder do not exhibit any memory effects.[38]

2. In the second scenario, the single molecule system undergoes a dynamic process governed by operator $\mathcal{L}$, which gives rise to the nonexponential waiting time, $Q(t) = \langle j|\exp[-\mathcal{L}t]|i\rangle$. For a linear operator, the waiting time distribution assumes the same functional form as the static disorder, $Q(t) = \Sigma_i \rho_i \exp(-\lambda_i t) = \int \rho(\lambda) \exp(-\lambda t)$, where λ is the eigenvalue of the linear operator L. In this case, each transition follows the nonexponential waiting time distribution $Q(t)$, although statistically we cannot differentiate it from the first scenario. Diffusion-controlled charge transfer[39,40] or, generally, diffusion-controlled reactions,[41] is an example of this scenario.

3. In the third scenario, the single molecule system samples a new rate constant generated from a rate distribution $\rho(k)$ and retains the rate for a sufficiently long time. Then, the system exhibits a single exponential decay for this transition within a reasonable experimental window and measurements averaged over many windows or over many molecules are inhomogeneous, giving $\langle A[K(t)]\rangle = \int A[t, k]\rho(k)\, dk$. This type of disorder cannot be rigorously described by $Q(t)$ and exhibits strong correlations between different measurements, e.g., correlations between fluorescence lifetime and intensity distribution. In a sense, we can view this scenario as the slow modulation limit of conformational fluctuations, i.e., slow on the experimental time-scale.

4. The last scenario is concerned with conformational fluctuations, multiple emission states, and multiple detection probes. These are different physical realizations of nonrenewal kinetics that can be formulated in a uniform language. The present formalism is developed for renewal processes, but can be extended to nonrenewal processes by writing the first passage time distribution as a tensor, which can be used to predict memory effects such as correlations between emission lifetimes, intensity, and yields. We have kept a particular order of Q's in eqs 36 and 51, which is irrelevant for the current scalar analysis but becomes important in the generalization to the tensor version. These issues have been studied extensively for rate processes and will be formulated in detail for continuous waiting time distributions in a future publication.[8]

Similar to on−off statistics in enzymatic turnover reactions, the correlation between photon emission events (lifetime and intensity) provides insight into the emission state(s) and the possible interconversion between these states. As illustrated in Figure 6, there are three possible generic schemes of photon

emission kinetics in single molecule blinking.

• In the case of a single emission state, as described in Figure 6a, with the possible presence of the triplet state, the photon emission is a renewal process as described in this article. As a result, there will be no correlations between two photon lifetime measurements, between two fluorescence intensities, or between lifetime and intensity.

• In the case of one emission state and one dark state, as in Figure 6b, interconversion between the two states is modulated by a hidden process. If the interconversion is much slower than the emission lifetime, there will be correlations between intensity measurements at different times, but there will be no correlation between different emission lifetime measurements.

• In the case of two or more modulated emission states with or without the dark state, as in Figure 6c, there will be correlations in intensity, in lifetime, and between intensity and lifetime. As discussed in a recent paper,[17] this type of correlation is due to memory effects and is different from the photon correlation measured by the Poisson indicator.

Experimental evidence from emission lifetime measurements and from fluorescence intensity measurements suggests case (c) for quantum dot blinking kinetics,[42−44] although the nature of emission states remains unclear. Here, we classify possible kinetic schemes responsible for blinking phenomena into the three generic schemes in Figure 5 without determining underlying physical mechanisms. The experimental observation of power-law waiting time distribution in quantum dots blinking[45−48] and its physical interpretations[39,49] are beyond the scope of the current discussion and will be addressed elsewhere.

VII. Concluding Remarks

In this paper, we introduce the concept of the generic scheme: an irreducible scheme that cannot be further simplified, given experimental probes and prior knowledge, i.e., a scheme with the minimal number of necessary links associated with waiting time distributions. The implications of this concept are 2-fold. (1) When a subscheme along the "backbone" or "skeleton" is modified, the irreducible generic scheme is topologically invariant and the formal expressions for single molecule measurements retain the same functional form but with a different waiting time distribution for the modified subscheme. (2) The irreducible generic scheme imposes a limit on the amount of information from single molecule experiments: One must not overinterpret the irreducible generic scheme from the data, because different kinetic subschemes can lead to the same waiting time distribution. Often, additional measurements are required to assign explicit physical meaning to the resolved waiting time distributions. On the basis of these two considerations, we conclude that the irreducible generic scheme is the maximal scheme for analyzing single molecule data, but also the minimal scheme for solving a more complex kinetic problem.

The reduction to the irreducible generic scheme is carried out using two kinetic motifs, sequential and branching, and the corresponding expressions in eqs 32 and 33, respectively. A complex kinetic scheme often involves several motifs, locally or globally, which may not be directly resolved from single molecule measurements. Following the single molecule reaction pathway(s), we are able to derive self-consistent pathway expressions for the first passage time distribution(s), $\phi(t)$, and thus obtain all other single molecule measurements. Each kinetic loop, including a reversible link along the kinetic pathway, defines a self-consistent equation, which is a convolution of waiting time distributions associated with each link and first passage time distribution(s) associated with relevant states. Our self-consistent pathway solution is essentially the same as the transfer matrix solution but is transferable to different variations of the irreducible generic scheme, thus providing flexibility in incorporating kinetic modifications. For example, enzymatic turnover and fluorescence emission are analyzed systematically and are found to share the same generic scheme composed of a monitored link, controlled link, and unknown link, each representing a simple elementary kinetic step or a complex kinetic subscheme. The calculation of the first passage time distribution lays the basis for computing all single molecule quantities, including distribution of a sequence of events, interevent correlation, and event number distribution, which are discussed in detail in Sec. II. As a result, various measurements, including turn-over rate, emission lifetime, and fluorescence intensity, are computed using eqs 36 and 51. Possible scenarios of nonexponential waiting time distributions and their consequences on observed fluorescence intensity distribution, lifetime distribution, and their correlations are discussed in the context of blinking mechanisms.

In a different context, Ross and his collaborators have pioneered the pulsed concentration response method and correlated metric construction to deduce complex reaction mechanisms.[50−52] In the linear response regime, these measurements are equivalent to the first-order kinetics described in this article. Thus, the concept of the generic scheme can be applied to systematically reconstruct the connectivity in a complex kinetic scheme using these response and correlation measurements. For example, our solution for the first passage time distribution, $\phi_{ij}(t)$, in particular eq 46 for chain reactions, predicts the response profile at the ith state induced by a pulse at the jth state, giving both the peak and its position. In Appendix C, we explore the short-time behavior of the waiting time distribution as a tool to reveal the causal connectivity of the underlying chemical network responsible for $\phi(t)$.

In the spirit of this work, we will extend the formulation of generic schemes to a tensor notation[8] adequate for multiple emission states and/or multiple conformational channels, and classify the information provided by various single molecule measurements on the basis of generic schemes in order to provide guidelines for the analysis and interpretation of single molecule data.

Acknowledgment. We thank Attila Szabo for his suggestions about the manuscript, John Ross for the discussion of Appendix C, and both reviewers for valuable comments. The work is supported by NSF grants CHE0556268, CHE0806266, and a Dreyfus Teacher-Scholar Award.

Appendix A. Equivalence between the Rate Formalism and Waiting Time Formalism

Single molecule kinetic schemes are first-order rate processes by definition and were first formulated in terms of rate matrices, as shown in section IIA. In comparison, the waiting time distribution formalism in section IIB renders much flexibility in analyzing complex kinetic schemes. In fact, exponential rate processes can be considered as a special case of general waiting time distribution processes, whereas the more complex waiting time distribution processes can always be decomposed into a set of first-order rate processes. Therefore, we expect that the two formalisms in sections IIA and IIB are equivalent and will demonstrate this equivalency for the basic single molecule measurements in Figure 1.

• The first step is to identify the waiting time distribution function $Q_{ij}(t)$ for a rate step as $Q_{ij}(t) = k_{ij} \exp(-k_j t)$ or

$$Q_{ij}(s)=\frac{k_{ij}}{s+k_j}=\left[K\frac{1}{Is+K_D}\right]_{ij} \tag{65}$$

The rate matrix is $K = K_D - K_{OD}$, where $K_{D,ij} = \delta_{ij}k_j$ is the diagonal part of the rate matrix and $K_{OD,ij} = (1 - \delta_{ij})k_{ij}$ is the off-diagonal part of the rate matrix. Using $Q_{ij}(s)$ in eq 65, we evaluate the adjacent event distribution function in eq 2 explicitly, giving

$$\begin{aligned}\phi(s)&=Q'_{ij}(s)\left[\frac{1}{I-Q_0(s)}\right]_{ji}\\&=\left[K'\frac{1}{sI+K_D}\right]_{ij}\left[\frac{1}{I-K_{0,OD}/(sI+K_D)}\right]_{ji}\\&=K'_{ij}\left[\frac{1}{sI+K_D-K_{0,OD}}\right]_{ji}=K'_{ij}\left[\frac{1}{s+K_0}\right]_{ji}\end{aligned} \tag{66}$$

which recovers eq 17. Here, the monitored transition rate K' contributes to off-diagonal terms, so that $K_{0,OD} = K_{OD} - K'$ and $K_0 = K_D - K_{0,OD}$ are the rate matrices excluding the monitored transition. Similarly, we can show

$$\psi(s)=Q'_{ij}(s)\left[\frac{1}{I-Q(s)}\right]_{ji}=K'_{ij}\left[\frac{1}{sI+K}\right]_{ji} \tag{67}$$

with $K = K_D - K_{OD}$, and, consequently, the equivalence for $f_{ev,m}$ and $g_{ev,m}$.

• The key in demonstrating the equivalence between eqs 4 and 19 is the survival probability $S(t)$, which is expressed in terms of rates as $S(s) = \Sigma_l G_{li}(s)$ and in terms of $Q(t)$ as $S(s) = [1 - \phi(s)]/s$. Using the rate expression for $\phi(s)$ in Eq. (2), we have

$$S(s)=\frac{1}{s}\left[1-K'_{ik}\left(\frac{1}{sI+K_0}\right)_{ki}\right]=\frac{1}{s}\sum_{lj}(sI+K_0-K')_{lj}\times\left(\frac{1}{sI+K_0}\right)_{ji}=\sum_l[G_0(s)]_{li} \tag{68}$$

where $\Sigma_l K_{lj} = 0$ is used. A related quantity is the average first passage time, defined as $\langle\tau\rangle = \phi(0) = \Sigma_l[K_0^{-1}]_{li}$. We note that, for the stationary solution, $K\rho = (K_0 - K')\rho = 0$, or, equivalently, $\rho = K_0^{-1}K'\rho$. Summation over the both sides of the expression leads to

$$1=\sum_l[K_0^{-1}]_{li}K'_{ij}\rho_j=\langle t\rangle K'_{ij}\rho_j \tag{69}$$

which yields the average rate $\langle t\rangle^{-1} = K'_{ij}\rho_j$.

• A more difficult task is to derive the probability of the first monitored transition in the time-averaged initial condition, $\tilde{\phi}$, which is defined with $Q(s)$ in eq 30 or with rate constants in eq 13. The PDF can also be rewritten in a different form as

$$\bar{\phi}(s)=\sum_l K'_{ij}G_{0,jl}(s)\rho_l=\sum_{kl}[-(sI+K)+(sI+K_0)]_{kj}\times\left[\frac{1}{sI+K_0}\right]_{jl}\rho_l=\sum_{kl}[-sG_0(s)+I]_{kl}\rho_l=\mathcal{LT}\left[\sum_{kl}\dot{G}_{0,kl}(t)\rho_l\right] \tag{70}$$

Thus, the PDF of the first event is the depletion rate of the equilibrium distribution due to the sink K'_{ij}, i.e., $\tilde{\phi}(t) = -\Sigma_{kl}\dot{G}_{0,kl}\rho_l$, which is intuitively easy to understand. As a result of eq 70, we can rewrite eq 30 as

$$\begin{aligned}\bar{\phi}(t)&=\sum\left[-\frac{s}{sI+K_0}+I\right]\rho=\sum\frac{1}{sI+K_0}(K+K')\rho\\&=\sum G_0(s)K'\rho\end{aligned} \tag{71}$$

where Σ represents summations over both the final and initial states. On the other hand, using eq 69, we rewrite eq 13 as

$$\bar{\phi}(t)=\frac{\sum_l G_{0,li}}{\langle t\rangle}=\sum G_0(s)K'\rho \tag{72}$$

thus demonstrating the equivalence between eqs 30 and 13.

Appendix B. Time Averaged Initial Condition and Poisson Indicator

We limit our formulation in section II to event-averaged single molecule quantities and will include here a brief discussion of time-averaged quantities including the Poisson indicator. The key difference between the two counting conditions is the first event, which is selected randomly along the time axis in time-averaged initial condition. Thus the probability of the first event is special is given by $\tilde{\phi}$ defined in eq 30 and the PDF of a sequence is defined in eq 31. As a result, and the probability distribution is given by

$$P(N,t)=\left[\prod_{i=1}^{N}\int_{t_{i-1}}^{t}\mathrm{d}t_i\right]S(t-t_N)f_N(t_1,t_2,\cdots,t_N) \tag{73}$$

except for the special case of $P(0, t)$. The simplest way to obtain an expression for $P(0, t)$ is via the normalization condition, $\Sigma_{N=0}^{\infty} P(N, t) = 1$, which in combination with eq 73 yields in Laplace space

$$P(0,s)=\frac{1}{s}-\sum_{N=1}^{\infty}P(N,s)=\frac{1}{s}\left[1-\frac{S(s)}{\langle t\rangle}\right] \tag{74}$$

With $P(N, t)$, we can evaluate all the moments $\langle N(t)^n\rangle = \Sigma_{N=0}^{\infty} P(N, t)N^n$, e.g.

$$\mathcal{LT}\langle N(t)\rangle=\frac{1}{s^2\langle t\rangle} \tag{75}$$

and

$$\mathcal{LT}\langle N^2(t)\rangle=\frac{1+\varphi(s)}{1-\varphi(s)}\frac{1}{s^2\langle t\rangle} \tag{76}$$

A simple approximation to evaluate $P(N, t)$ is to assume a Gaussian distribution and use the above two moments to obtain

$$P(N,t)\approx 1/\sqrt{2\pi\Delta(t)}\exp\left(-\frac{[N-\langle N\rangle]^2}{2\Delta(t)}\right) \tag{77}$$

with the variance $\Delta(t) = \langle N^2(t)\rangle - \langle N(t)\rangle^2$. Combining the first two moments, we also obtain the expression for the Poisson indicator often used in photon statistics analysis

$$\mathcal{LT}[\langle N(t)\rangle\mathcal{Q}(t)]=\frac{2}{s^2\langle t\rangle}\left[\frac{\phi(s)}{1-\phi(s)}-\frac{1}{s\langle t\rangle}\right]=\frac{2}{s^2\langle t\rangle}\left[\psi(s)-\frac{1}{s\langle t\rangle}\right] \tag{78}$$

where $\langle N(t)\rangle\mathcal{Q}(t) = \langle N(t)^2\rangle - \langle N(t)\rangle^2 - \langle N(t)\rangle$. Here, we use $\mathcal{Q}$ to denote the Poisson indicator to avoid confusion with the notation for the waiting time distribution function Q. The long time limit of the Poisson indicator defines Mandel's $\mathcal{Q}$ parameter, given as $\mathcal{Q}_M = \lim_{t\to\infty}\mathcal{Q}(t) = [\langle t^2\rangle - 2\langle t\rangle^2]/\langle t\rangle^2$, where the moments of lifetime are written as $\langle t^l\rangle = \int t^l\phi(t)\,\mathrm{d}t = (-1)^l\partial_s^l\phi(s$

$= 0$). The same result for the Mandel's parameter can be directly obtained from the small s-expansion, $\psi(s) = 1/s\langle t\rangle + \mathcal{Q}_M/2 + ...$ These results for the Poisson indicator have appeared earlier in literature.[14,17,19]

The other two types of measurements discussed in section II can also be evaluated with the time-averaged initial condition. In particular, the probability of detecting a monitored event with the time-averaged initial condition in a steady-state process is a constant, $g(t) = 1/\langle\tau\rangle$. It then follows that the multiple time number density in eq 22 becomes

$$g(t_1, t_2, \cdots, t_m) = \psi(t_m - t_{m-1}) \cdots \psi(t_2 - t_1)\frac{1}{\langle t\rangle} \quad (79)$$

and the counting cumulants in eq 24 becomes

$$\mathcal{LT}[C_m(t)] = \frac{m!\,\psi^{m-1}(s)}{s^2\langle t\rangle} \quad (80)$$

The definition for time-averaged probability $P(N, t)$ including the expression for $P(0, t)$ in eq 74 leads to the generating function

$$P(z, s) = \frac{1}{s}\left[1 - \frac{1-\phi(s)}{\langle t\rangle s}\frac{1-e^{iz}}{1-\phi(s)e^{iz\phi(s)}}\right] \quad (81)$$

from which moments can be derived and can be shown to be equivalent to cumulants in eq 80.

Appendix C. Initial Rise in Waiting Time PDF and Causal Connectivity in Chemical Kinetics

A complex chemical reaction is composed of multiple elementary reaction steps, leading to nonexponential behavior in the waiting time probability distribution function (PDF). In this appendix, we discuss a general relationship between the short time behavior of $\phi(t)$ and the causal connectivity of the underlying kinetic network: The initial rise of the waiting time distribution determines the number of elementary rate steps along the shortest pathway between any pair of states and is independent of multiple pathways or the mass rate law.

Let us consider a simple experimental measurement of the waiting time distribution: Given the stationary population at all state initially, we perturb the state 0 by introducing additional population, and then measure the response at state j. The deviation of average concentration at state j, $u_j = \rho_j - \rho_{s,j}$, from its stationary value $\rho_{s,j}$, follows the rate equation

$$\dot{u}_j = \sum_i k_{ji}u_i - \left(\sum_i k_{ij}\right)u_j \quad (82)$$

At short times, we can ignore the depletion from the probed state, because it has high-order time-dependence and thus write

$$u_j \approx \int_0^t \sum_i k_{ji}u_i\,dt \approx \sum_i k_{ji}tu_i \quad (83)$$

Iterating the above expression, we obtain

$$u_j \approx \sum[\prod k_{nm}t]u_0 \quad (84)$$

where the sum is taken over all the pathways between the initial state 0 and the probed state j and the product is taken for each step along a pathway. At short times, the deviation u is dominated by the shortest pathway, and the initial rise in the response function follows the algebraic law

$$\lim_{t\to 0}\phi(t) \propto \lim_{t\to 0}\psi(t) \propto k_L t^L \quad (85)$$

where exponent L is the minimal number of steps between the perturbed state and the probed state, and $k_L = \prod k_{nm}$ is the product of the rate coefficients along the shortest pathway. Thus, the initial arise of the waiting time distribution $\lim_{t\to 0}\phi(t) \propto t^L$ can be used to infer the shortest pathway between a pair of states, and a series of such measurements between different pairs of states can determine the causal connectivity of the underlying kinetic network.

The proposed experiment is in fact the pulsed concentration response method of Ross and co-workers[50,51] and has been analyzed extensively. But the initial-rise method has not been applied because it requires accurate short-time measurements, which are not feasible in bulk due to sensitivities to initial preparation and spontaneous fluctuations in concentration. However, the single molecule measurement of the waiting time (i.e., first passage time, dwelling time) is nonperturbative and does not require initial preparation or synchronization. Thus, fast and repetitive single molecule detection can in principle make it possible to use the proposed relationship of eq 85. It should be emphasized that eq 85 is not limited to linear kinetics as in single molecule measurements but applies in general to any linear and nonlinear kinetic networks.

Appendix D. Turnover Time for Chain Enzymatic Reactions

We first rearrange eq 48 in the following form

$$\langle t_n\rangle - \langle t_{n-1}\rangle = (\langle t_{n+1}\rangle - \langle t_{n-1}\rangle)q_n + \tau_n \quad (86)$$

with initial conditions $q_1 = 1$ and $\langle t\rangle_{L+1} = 0$. Introducing a new variable $b_n \equiv \langle t\rangle_{n+1} - \langle t\rangle_n$, we can rewrite eq 86 as

$$b_{n-1} = (b_n + b_{n-1})q_n + \tau_n \quad (87)$$

or equivalently

$$b_n = b_{n-1}\left(\frac{1}{q_n} - 1\right) - \frac{\tau_n}{q_n} \quad (88)$$

Iterating eq 88, we arrive an explicit solution

$$b_n = -\sum_{i=1}^{n-1}\frac{\tau_i}{q_i}\prod_{j=i+1}^{n}\left(\frac{1}{q_j} - 1\right) - \frac{\tau_n}{q_n} \quad (89)$$

with the initial condition $q_1 = 1$ and $b_1 = -\tau_1$. Finally, we notice that

$$\sum_{n=1}^{L} b_n = -\langle t_1\rangle + \langle t_{L+1}\rangle = -\langle t_1\rangle \equiv -\langle t\rangle \quad (90)$$

and immediately find the solution for the turnover time in eq 49.

References and Notes

(1) Bache, T.; Moerner, W. E.; Orrit, M.; Wild. U. P. *Single-molecule optical detection, imaging and spectroscopy*; VCH: Wienheim, Germany, 1996.

(2) Moerner, W. E.; Orrit, M. Illuminating single molecules in condensed matter. *Science* **1999**, *283*, 1670.

(3) van Kampen, N. G. *Stochastic processes in physics and chemistry*; Elsevier Science: New York, 1992.

(4) Ball, F. G.; Rice, J. A. Stochastic models for ion channels: introduction and bibliography. *Math. Biosci.* **1992**, *112*, 189, and references within.

(5) Witkoskie, J.; Cao, J. Single molecule kinetics i. analysis of indicators. *J. Chem. Phys.* **2004**, *121*, 6361.

(6) Bruno, W. J.; Yang, J.; Pearson, J. E. Using independent open-to-closed transitions to simplify aggregated markov models of ion channel gating kinetics. *Proc. Natl. Acad. Sci. U.S.A.* **2005**, *102*, 6326.

(7) Flomenbom, O.; Silbey, R. J. Utilizing the information content in two-state trajectories. *Proc. Natl. Acad. Sci. U.S.A.* **2006**, *103*, 10907.

(8) For a review and a list of relevant articles on modulated reactions, i.e., non-renewal processes, we refer readers to the sequel of the present paper, i.e., paper 2.

(9) Ninio, J. Alternative to the steady-state method: Derivation of reaction rates from first-passage times and pathway probabilities. *Proc. Natl. Acad. Sci. U.S.A.* **1987**, *84*, 663.

(10) Feller. W. *An introduction to probability theory and its applications*; Wiley: New York, 1970.

(11) Flomenbom, O.; Klafter, J. *Phys. Rev. Lett.* **2005**, *95*, 098105.

(12) Flomenbom, O.; Silbey, R. J. Path probability density functions for semi-markovian random walks. *Phys. Rev. E* **2007**, *76*, 041101.

(13) Barkai, E.; Jung, Y.; Silbey, R. Theory of single-molecule spectroscopy. *Annu. Rev. Phys. Chem.* **2004**, *55*, 457.

(14) Gopich, I. V.; Szabo, A. Theory of the statistics of kinetic transitions with application to single molecule enzyme catalysis. *J. Phys. Chem.* **2006**, *124*, 1.

(15) Cao, J. Event-averaged measurements of single molecule kinetics. *Chem. Phys. Lett.* **2000**, *327*, 38.

(16) Gopich, I. V.; Szabo, A. Statistics of transitions in single molecule kinetics. *J. Chem. Phys.* **2003**, *118*, 454.

(17) Cao, J. Correlation in single molecule photon statistics: Renewal indicator. *J. Phys. Chem. B* **2006**, *110*, 19040. Note the notational differences: (1) The multiple-time number density is denoted as $g(t,.\ .)$ in the present paper instead of $f(t,.\ .)$ in the referred paper. (2) The number of monitored transitions is denoted as $N(t)$ in the present paper instead of $n(t)$ in the referred paper.

(18) Gopich, I. V.; Szabo, A. Theory of photon statistics in single-molecule forster resonance energy transfer. *J. Chem. Phys.* **2005**, *122*, 014707.

(19) Jung, Y.; Barkai, E.; Silbey, R. A stochastic theory of single molecule spectroscopy. *Adv. Chem. Phys.* **2002**, *123*, 199.

(20) Witkoskie J.; Cao. J. Signatures of detailed balance violations in single molecule event statistics. 2008. submitted.

(21) Lerch, H. P.; Rigler, R.; Mikhailov, A. S. Functional conformational motions in the turnover cycle of cholesterol oxidase. *Proc. Natl. Acad. Sci. U.S.A.* **2005**, *102*, 10807.

(22) Velonia, K.; Flomenbom, O.; Loos, D.; Masuo, S.; Cotlet, M.; Engelborghs, Y.; Hofkens, J.; Rowan, A. E.; Klafter, J.; Nolte, R. J. M.; de Schryver, F. C. Single enzyme kinetics of calb catalyzed hydrolysis. *Angew. Chem., Int. Ed.* **2005**, *44*, 560.

(23) English, B. P.; Min, W.; van Oijen, A. M.; Lee, K. T.; Luo, G.; Sun, H.; Cherayil, B. J.; Kou, S. C.; Xie, X. S. Ever-fluctuating single enzyme molecules: Michaelis-menten equation revisited. *Nat. Chem. Biol.* **2006**, *2*, 2.

(24) Bar-Haim, A.; Klafter, J. On mean residence and first passage times in finite on-dimensional systems. *J. Chem. Phys.* **1998**, *109*, 5187.

(25) Kolomeisky, A.; Fisher, M. F. Extended kinetic models with waiting-time distributions: exact solutions. *J. Chem. Phys.* **2000**, *113*, 10867.

(26) Tsygankov, D.; Linden, M.; Fisher, M. E. Back-stepping, hidden substeps, and conditional dwell times in molecular motors. *Phys. Rev. E* **2007**, *75*, 021909.

(27) Chemla, Y. R.; Moffitt, J. R.; Bustamante, C. Exact solutions for kinetic models of macromolecular dynamics. *J. Phys. Chem.* 2008.

(28) Fleury, L.; Segura, J.; Zumofen, G.; Hecht, B.; Wild, U. P. Nonclassical photon statistics in single-molecule fluorescence at room temperature. *Phys. Rev. Lett.* **2000**, *84*, 1148.

(29) Molski, A.; Hofkens, J.; Gensch, T.; Boens, N.; De Schryver, F. Theory of time-resolved single-molecule fluorescence spectroscopy. *Chem. Phys. Lett.* **2000**, *318*, 325.

(30) Lippitz, M.; Kulzer, F.; Orrit, M. Statistical evaluation of single nano-object fluorescence. *ChemPhysChem* **2005**, *6*, 770.

(31) Plakhotnik, T.; Donley, E. A.; Wild, U. P. *Annu. Rev. Phys. Chem.* **1997**, *49*, 181.

(32) Osad'ko. I. S. *Selective spectroscopy of single molecules*; Springer Series in chemical physics; Springer: Berlin, 2002.

(33) Chernyak, V.; Sanda, F.; Mukamel, S. Coherence and correlations in multiple quantum measurements of stochastic quantum trajectories. *Phys. Rev.* **2006**, *E73*, 036119.

(34) Makarov, D.; Metiu, H. Control, with an rf field, of photon emission times by a single molecule and its connection to laser-induced localization of an electron in a double well. *J. Chem. Phys.* **2001**, *115*, 5989.

(35) Mandel L. and Wolf. E. *Optical coherence and quantum optics*; Cambridge University Press: New York, 1995.

(36) Xie, X. S.; Trautman, J. K. Optical studies of single molecules at room temperature. *Annu. Rev. Phys. Chem.* **1998**, *49*, 441.

(37) Barbara, P.; Gesquiere, A. J.; Park, S. J.; Lee, Y. J. Single-molecule spectroscopy of conjugated polymers. *Acc. Chem. Res.* **2005**, *602*, 38.

(38) Cao, J. Single molecule waiting time distribution functions in quantum processes. *J. Chem. Phys.* **2001**, *114*, 5138.

(39) Tang, J.; Marcus, R. A. Diffusion-controlled electron transfer processes and power-law statistics of fluorescence intermittency of nanoparticles. *Phys. Rev. Lett.* **2005**, *95*, 107401.

(40) Tang, J.; Marcus, R. A. Mechanisms of fluorescence blinking in semiconductor nanocrystal quantum dots. *J. Chem. Phys.* **2005**, *123*, 054704.

(41) Wang, J.; Wolynes, P. Intermittency of activated events in single molecules: The reaction diffusion description. *J. Chem. Phys.* **1999**, *110*, 4812.

(42) Neuhauser, R. G.; Shimuzu, K. T.; Woo, W. K.; Empedocles, S. A.; Bawendi, M. G. Correlation between fluorescence intermittency and spectral diffusion in single semiconductor quantum dots. *Phys. Rev. Lett.* **2000**, *85*, 3301.

(43) Labeau, O.; Tamarat, P.; Lounis, B. Temperature dependence of the luminescence lifetime of single cdse/zns quantum dots. *Phys. Rev. Lett.* **2003**, *90*, 257404.

(44) Zhang, K.; Chang, H.; Fu, A.; Alivisatos, A. P.; Yang, H. Continuous distribution of emission states from single cdse/zns quantum dots. *Nano Lett.* **2006**, *6*, 843.

(45) Kuno, M.; From, D. P.; Hamann, H. F.; Gallagher, A.; Nesbitt, D. J. Nonexponential blinking kinetics of single cdse quantum dots: A universal power law behavior. *J. Chem. Phys.* **2000**, *112*, 3117.

(46) Shimizu, K. T.; Neuhauser, R. G.; Leatherdale, C. A.; Empedocles, S. A.; Woo, W. K.; Bawendi, M. G. Blinking statistics in single semiconductor nano-crystal quantum dots. *Phys. Rev. B* **2001**, *73*, 205316.

(47) Margolin, G.; Protasenko, V.; Kuno, M.; Barkai, E. Photon counting statistics for blinking cdse-zns quantum dots: A levy walk process. *J. Phys. Chem. B* **2006**, *110*, 19053.

(48) Chung, I.; Witkoskie, J.; Cao, J.; Bawendi, M. Fluorescence intensity time traces of collections of cdse nanocrystals qds. *Phys. Rev. E* **2006**, *73*, 011106.

(49) Cichos, F.; von Borczskowski, C.; Oritt, M. Power-law intermittency of single emitters. *Curr. Opin. Colloid Interface Sci.* **2007**, *12*, 272.

(50) Ross, J. New approaches to the deduction of complex reaction mechanisms. *Acc. Chem. Res.* **2003**, *36* (11), 839.

(51) Vance, W.; Arkin, A.; Ross, J. Determination of causal connectivities of species in reaction networks. *Proc. Natl. Acad. Sci. U.S.A.* **2002**, *99* (9), 5816.

(52) Vlad, M. O.; Arkin, A.; Ross, J. Response experiments for nonlinear systems with application to reaction kinetics and genetics. *Proc. Natl. Acad. Sci. U.S.A.* **2004**, *101* (19), 7223.

JP803347M